Nanoscale

Accepted Manuscript

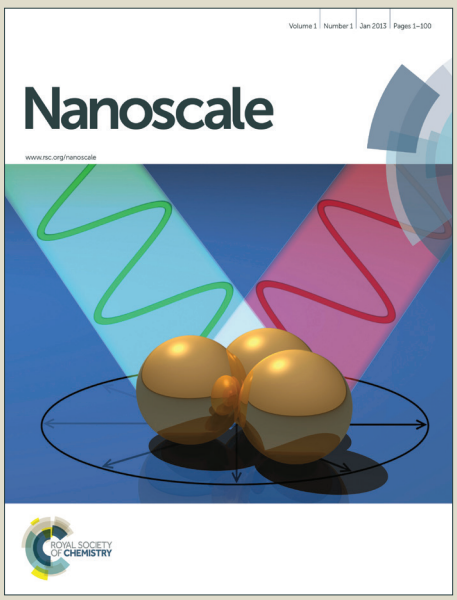

ROYAL SOCIETY OF CHEMISTRY

www.rsc.org/nanoscale

A Dual-functional Asymmetric Squaraine-based Low Band Gap Hole Transporting Material for Efficient Perovskite Solar Cells

Sanghyun Paek[1,2], Malik Abdul Rub,[3] Hyeju Choi[2], Samia A. Kosa,[3] Khalid A. Alamry,[3] Jin Woo Cho[4], Peng Gao*[1], Jaejung Ko *[2], Abdullah M. Asiri,[3] Mohammad Khaja Nazeeruddin*[1],

[1]Group for Molecular Engineering of Functional Materials, Laboratory of Photonics and interfaces, Institute of Chemical Sciences and Engineering, Ecole polytechnique fédérale de Lausanne, CH-1951 Sion, Switzerland. E-mail: mdkhaja.nazeeruddin@epfl.ch; peng.gao@epfl.ch

[2] Department of New Material Chemistry, Korea University, Jochiwon, Chungnam 339-700, Korea. E-mail: jko@korea.ac.kr

[3]Center of Excellence for Advanced Materials Research (CEAMR), King Abdulaziz, University, Jeddah, Saudi Arabia.

[4] LG Innotek QE team 570, Hyuanm-ro, Munsan-eup, Paju-si, Gyeongi-do 413-901, Republic of Korea

Abstract.

We demonstrate for the first time asymmetric squaraine-based low band-gap hole transporting material, which acted as both light harvesting and hole transporting layers methylammonium lead triiodide perovskite solar cells. Opto-electrochemical characterization revealed extremely high molar extinction coefficient of the absorption bands in the low energy region and prominent space charge delocalization due to its electronically asymmetric nature. Suitable band alignment of the squaraine HOMO level with the valence band edge of the perovskite, and conduction band of the TiO_2 with LUMO of the perovskite allowed cascade of hole extraction and electron injection, respectively. Red-shifted absorption was observed for both HTMs in thin films coated on perovskite, and the optimized devices exhibited an

impressive PCE of 14.7 % under full sunlight illumination (100 mW cm-2, AM1.5 G). The efficiency value is comparable to that of the devices using a state-of-the-art spiro-OMeTAD hole transport layer under similar conditions. Ambient stability after 300 h revealed that 88% of the initial efficiency remained for JK216D, and almost no change with JK217D, indicating the devices had good long-term stability and thus suggesting that the asymmetric squaraines have great potential as dual-functional HTM for high performance perovskite solar cells.

Introduction.

As a new class of solution-processable light absorbing material, methylammonium lead triiodide perovskite has attracted prevailing attention from material and photovoltaic communities.[1,2] The power conversion efficiency (PCE) of solid-state perovskite solar cells (PSCs) has been quickly increased from 3.9 to 20.1% as certified by National Renewable Energy Laboratory (NREL)[3] due to their intrinsic advantages like broad absorption in the visible regions,[4] high absorption coefficient,[5] high charge carrier mobility[6] and long diffusion length.[7] The n-i-p configuration of PCSs device inherited from the solid state dye-sensitized solar cells (ssDSC), a p-type semiconductor as hole transporting material (HTM) is one of the most critical components in the PCSs.[8] The 2,2',7,7'-tetrakis(N,N-di-p-methoxyphenylamine)-9,9'-spirobifluorene (spiro-OMeTAD) is by far the most studied and used molecular p-type HTM with the recently reported PCE of 19.7%.[9] Similar to spiro-OMeTAD, a large series of triphenylamine (TPA)-based small molecules and polymers have been reported as alternative HTMs in PSCs.[10–14] In most of these devices, these HTMs were wide bandgap semiconductors similar to spiro-MeOTAD, with absorption in the UV, and almost no absorption in the visible and near-IR regions of the solar spectrum as the neutral form. In this case the perovskite layer functions as the light absorber and the HTM layer is only responsible for hole transportation. Until recently, only limited number of low band gap

organic semiconductors have been used as HTMs in $CH_3NH_3PbX_3$-based PSCs, including donor–acceptor (D-A) polymers,[15–17] (A-)D-A-type oligomers[18–20] and substituted phthalocyanine.[21] Although there has been no report about the light absorption contribution from these low bandgap polymers, our group has found that with some visible to near-infrared light absorbing molecular HTMs, significant improvement of the photocurrent in the blue or red regions were observed respectively, which is in agreement with absorption of the corresponding HTM films.[18,22] This indicates a synergistic and effective participation of these HTMs as light absorbers together with perovskite over the solar spectrum.

Squaraines are promising class of pigments with a zwitterionic resonance structure and have found applications in areas such as imaging, nonlinear optics, photovoltaics, photodynamic therapy, and ion sensing,[23] due to their extremely high molar extinction coefficients ($\varepsilon > 10^5$ $L \cdot mol^{-1} \cdot cm^{-1}$ at 650 nm) and intense absorption in the near infrared (NIR) region of the solar spectrum.[24,25] It has been reported that upon modification, squaraine can be used as complementary absorber in dye sensitized solar cells (DSSC) [26,27] due to its ability to efficiently convert the low-energy (•1.4 eV) photons into electricity.[28] At the same time, squaraines have been reported to have p-type semiconductive properties and exhibit field-effect hole mobilities of ~ 10^{-5} to 1.3 $cm^2 V^{-1} s^{-1}$,[25,29] which indicates that squaraines pigments could behave as dual function of light harvesting and hole transporting layers.

In this work, we report the synthesis and characterization of two D-A-D-A-type low bandgap molecular semiconductor **JK216D** and **JK217D** based on asymmetric squaraine chromophore and for the first time their use as HTMs in perovskite solar cells and mesoporous TiO_2 as selective contact of electron. The devices having the structure of FTO/compact layer TiO_2/mesoporous TiO_2/$CH_3NH_3PbI_3$/HTM/Au fabricated. The optimized devices based on these new HTMs showed similar PCEs of up to 14.7%, which is slightly

lower compared to the value of 15.3% from spiro-OMeTAD. As a result of strong absorption in the visible and near-infrared region, we observed again the contribution from HTM layer to the photocurrent generated from the perovskite solar cells. These squaraine based HTM showed excellent stability with 12% loss in PCE with **JK216D** and almost no change with **JK217D** over 300 hours.

Experimental

Preparation of the squaraine based HTM molecules

The synthetic route of unsymmetrical squaraine HTM by stepwise condensation reaction of different heterocyclic moieties with central squaric acid is shown in Scheme S1. Half squaraine **1** and **2** were prepared by using the reported literature method.[30] Then they were condensed with **3** to yield **4** and **5** and induce a panchromatic absorption. Suzuki coupling of **4** and **5** with 5-formyl thiophene-2-boronic acid in THF/H_2O produced aldehyde **6** and **7**. These precursors were further condensed with hexyl 2-cyanoacetate to afford final compound as **JK-216D** and **JK-217D**. (Figure 1) The chemical structures of the synthesized products were verified by $^{1}H/^{13}C$ NMR spectroscopy and mass spectrometry. Additional details are given in the SI.

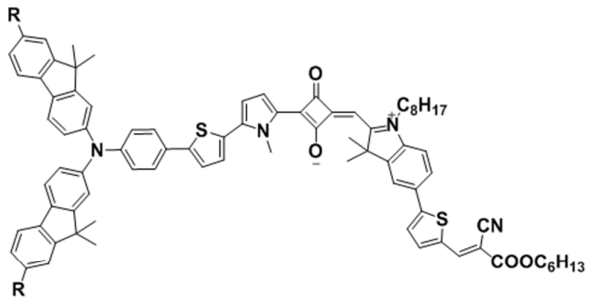

JK-216D: R = H
JK-217D: R = OC_6H_{13}

Figure 1. Chemical structures of the new HTM **JK-216D** and **JK-217D**.

Characterization

^{1}H and ^{13}C NMR spectra were recorded on a Varian Mercury 300 spectrometer. Elemental analyses were performed with a Carlo Elba Instruments CHNS-O EA 1108 analyzer. Mass spectra were recorded on a JEOL JMS-SX102A instrument. The absorption and photoluminescence spectra were recorded on a Perkin-Elmer Lambda 2S UV-visible spectrometer and a Perkin LS fluorescence spectrometer, respectively.

Fabrication of solar cells

FTO glass plates (Pilkington, TEC-8) were cleaned in a detergent solution using an ultrasonic bath for 30 min, rinsed with water and ethanol. The compact TiO_2 layer was deposited on the etched F-doped tin oxide substrate by spray pyrolysis at 450°C, using titanium diisopropoxide bis(acetylacetonate) solution. The FTO glass plates were immersed in 40 mM $TiCl_4$ (aqueous) at 70 °C for 30 min and sintered at 500 °C for 30 min. Mesoporous TiO_2 films was deposited by spin coating of a diluted TiO_2 paste (Dyesol 18NR-T, 1:3.5w/w diluted with ethanol) at 5000 rpm for 30s. The films were sintered at 500°C. PbI_2 was purchased from Aldrich and CH_3NH_3I was prepared similarly to a previously published method.[31] PbI_2 and CH_3NH_3I were added to a 250 mL flame-dried 2-neck round-bottom flask with γ-butyrolactone (GBL). The reaction mixture was heated to 100°C for 30 min. The reaction mixture was then cooled to room temperature. Then, the solvent removed and product was washed with hexane to obtain the $CH_3NH_3PbI_3$. The $CH_3NH_3PbI_3$ was stirred in a mixture of γ-butyrolactone (GBL) and dimethyl sulfoxide (DMSO) (7:3 v/v) at 60 ^{o}C for 12 h.[32] The $CH_3NH_3PbI_3$ solution was spin-cast on top of TiO_2/FTO substrate at 3000 rpm. For deposition of HTM layers, **JK-216D**/chlorobenzene (20 mM), **JK-217D**/chlorobenzene (20 mM) and **SpiroOMeTAD**/chlorobenzene (60 mM) solutions were prepared with two additives. 3.5 μL lithium bis(trifluoromethanesulonyl)imide (Li-TFSI)/acetonitrile (520 mg/1 mL) and 8.0 μL (4-tert-butylpyridine) (TBP) were added to the HTM/chlorobenzene solutions

as additives. The HTMs were spin-cast on top of the $CH_3NH_3PbI_3/TiO_2$/FTO substrate at 3000 rpm. Finally, a ~60 nm thick Ag electrode was deposited on top of the film under reduced pressure (lower than 10^{-6} Torr).

Results and discussion

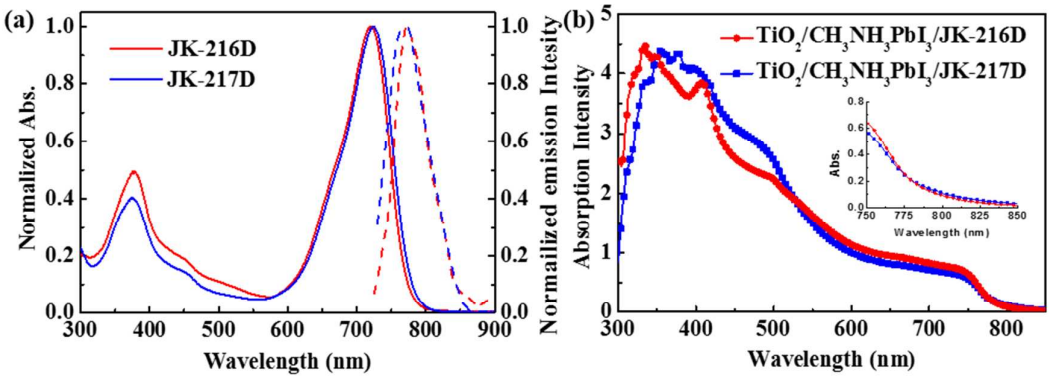

Figure 2. (a) UV-vis absorption and fluorescence spectra of **JK-216D** (red line) and **JK-217D** (blue line) in chlorobenzene. (b) UV-vis absorption spectra of $TiO_2/CH_3NH_3PbI_3$/HTM film. (inset: enlarged NIR region showing the absorption enhancement by HTM layers)

Based on the squaraine unit, strong electron donating and accepting groups were introduced to push the electronic absorption further to NIR region.[33] The UV-Vis absorption and emission spectra of **JK216D** and **JK-217D** in chlorobenzene (CB) are shown in Figure 2a. The **JK216D** and **JK-217D** exhibit almost identical absorption spectra with sharp absorption bands in the longer wavelength region 600–800 nm inside which high molar absorption coefficient of 119,000 M^{-1} cm^{-1} and 147,600 M^{-1} cm^{-1} were observed at 720 nm and 723 nm respectively. The spectrum of **JK217D** red shifted slightly as compared to **JK216D** due to increased electron donating ability after the substitution of hexlyloxy groups. The optical band gap (Eg) of **JK217D** and **JK216D** is calculated (1.66 and 1.65 eV) from the absorption

onset wavelength of the corresponding absorption spectrum respectively, which is to our knowledge one of the lowest bandgap HTMs ever used in perovskite solar cells.[20] (Table 1) It is expected that the strong absorption in the NIR region can harvest complementarily unabsorbed light passing through the perovskite layer. The fluorescence spectra show maximum emission at 772 nm and 770 nm for **JK216D** and **JK-217D**, with Stokes shifts of 52 nm and 47 nm respectively.

In Figure 2b, UV-Vis absorption spectra of both HTMs coated $CH_3NH_3PbI_3$ film are shown. The contribution of light absorption from of HTM layers coated on the perovskite can be seen from the fact that the absorption band of neat perovskite films is strongly enhanced, especially in the wavelength above 550 nm.[18] The enhancement in absorption of these sandwich films by the HTM layers resemble each other in the low energy region, the onset of which are extended up to 825 nm. This behaviour resemble the case when organic dyes absorbed on the TiO_2 surface and is attributed to the formation of J-aggregation as envisaged in the literature.[34]

Table 1. Optical, redox parameters of the new HTMs

Compounds	λ_{abs}[a]/nm (ε/$M^{-1}cm^{-1}$)	λ_{PL}[a]/nm	$E_{onset,\ ox}$ (V) / HOMO (eV)[b]	$E_{onset,\ red}$ (V) / LUMO (eV)[b]	E_{opt} (eV)[c]
JK-216D	378 (59,000), 720 (119,000)	772	0.21/-5.09	1.44/-3.44	1.65
JK-217D	376 (58,000), 723 (147,600)	770	0.21/-5.08	1.45/-3.43	1.66

[a] Absorption and emission spectra were measured in chlorobezene solution. [b] Redox potential of the compounds were measured in CH_2Cl_2 with 0.1M $(n\text{-}C_4H_9)_4NPF_6$ with a scan rate of 50 mVs^{-1} (*vs*. Fc/Fc^+). [c] E_{opt} was calculated from the absorption and emission cross peak in chlorobezene solution.

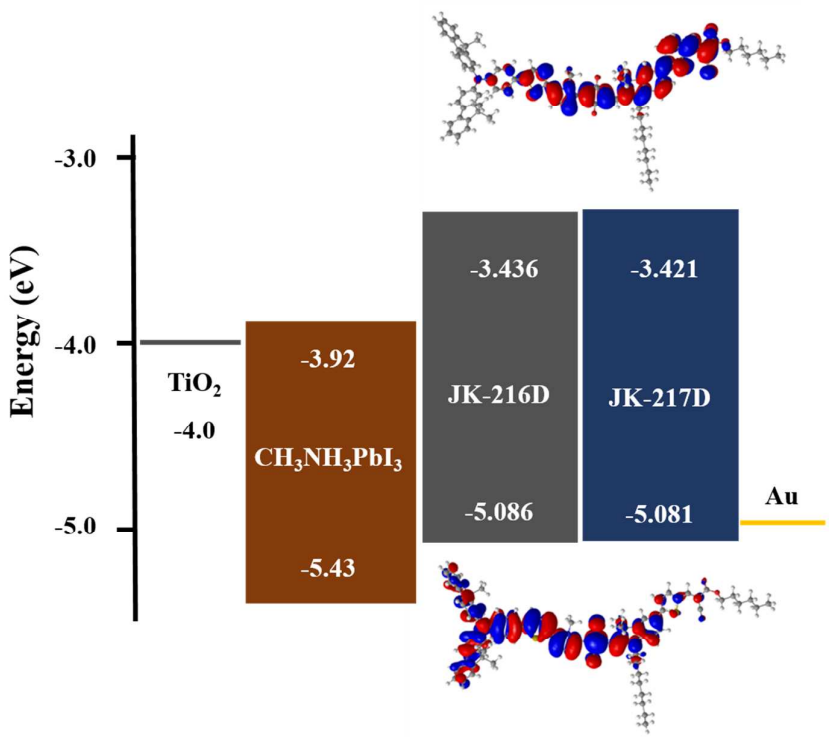

Figure 3. Energy level diagram of each component in a hybrid solar cell with isodensity surface plots of **JK-216D** as an reprehensive calculated by the time dependent-density functional theory (TD-DFT) using the B3LYP functional/6-31G* basis set.

Cyclic voltammograms (CV) of JK216D and JK-217D are shown in Fig. S1 and the parameters are summarized in Table 1. The two HTMs JK216D and JK-217D exhibited reversible oxidation processes with JK-217D having lower oxidation potential due to the extra hexyloxy substituents. The HOMO energy levels are calculated from the CV data with the assumption that the energy level of ferrocene is 4.8 eV below the vacuum level. No reduction potential was observed in the CV measurement. The HOMO levels of **JK216D** and **JK-217D** calculated from the onset oxidation potential are −5.09 eV and -5.08 eV respectively. As the HOMO energy level of $CH_3NH_3PbI_3$ is -5.43 eV,[35] the two new HTMs are energetically favorable for hole transfer. These trends are reflected in the energy level diagram and compared with the energy level of $CH_3NH_3PbI_3$ perovskite (Figure 3). The

LUMO energy level was estimated according $E_{LUMO} = E_{HOMO} - E_{0\text{-}0}$ to be -3.436 eV and -3.421 respectively, which will allow sufficient offset to the conduction band of perovskite to not only block the electrons from perovskite but also ensure cascade of electron transfer at the interface when the HTMs are excited.

Calculations using time dependent-density functional theory (TD-DFT) were used to investigate the electronic properties of the squaraine-based HTMs. As shown in Figure 3, the orbital density of the HOMO of representative **JK216D** locates on the bis-DMFA-thiophene-pyrrole core owing to its greater electron-donating strength, whereas the orbital density of LUMO was predominantly located between the squaraine and cyanoacrylate unit. The efficient intramolecular charge transfer leads to partial wave function overlap between LUMO and HOMO. A strong Coulomb interaction is induced, which will favor formation of neutral excitons and hole transport.[36]

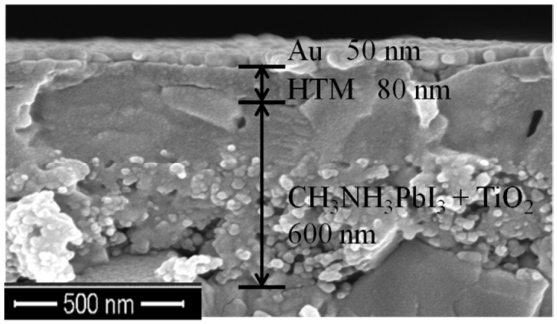

Figure 4. Cross-sectional SEM images of the $CH_3NH_3PbI_3$/HTM hybrid photovoltaic cells with JK-217D as HTM layer.

To evaluate the dual function of low band gap HTM on the performance of perovskite solar cells, various HTM materials including JK216D, JK-217D and spiro-OMeTAD were used for comparison. Cross-section SEM picture shown in Figure 4 illustrates a typical perovskite solar cell in which the $CH_3NH_3PbI_3$ perovskite layer was deposited on mesoporous-TiO_2 (m-

TiO_2) by a one-step deposition method as described in the experimental section. The perovskite penetrates into the m-TiO_2 and forms a capping-layer on top at the same time. The HTMs form a thin capping layer on the top of the smooth perovskite layer. The current-density-voltage (*J-V*) characteristics of optimized performance of three types of devices are shown in Figure 5(a). The device performance data is summarized in Table 2.

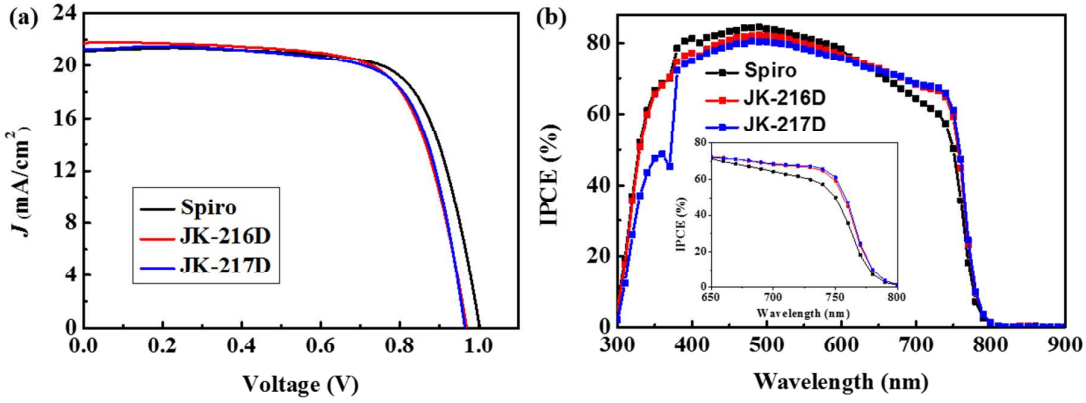

Figure 5. (a) Current (*J*)-voltage (*V*) curves of the solar cells with **JK-216D**, **JK-217D**, and Spiro under AM 1.5 conditions (100 mW/cm^2). (b) IPCE spectra of $CH_3NH_3PbI_3$/HTM perovskite solar cell.

As can be seen in the *J-V* curves, the reference cell with spiro-OMeTAD displayed a short-circuit current density (J_{SC}) of 21.105 mA cm^{-2}, a V_{OC} of 1002 mV, and a fill factor (FF) of 72.48%, resulting in a PCE of 15.33%, which is comparable with the state-of-the-art spiro-OMeTAD devices prepared under similar perovskite composition and device architecture.[37,38] Using **JK-216D** and **JK-217D** as HTMs, slightly increased J_{SC} of 21.754 and 21.226 mAcm^{-2} were observed respectively under standard global AM 1.5 illumination. However due to the relatively higher HOMO levels of **JK-216D** and **JK-217D**, their V_{OC} are decreased compared to that of spiro-OMeTAD. The fill factor of the device based on **JK-217D** is higher (71.94 %) compared to the device based on **JK-216D** (69.92 %), which could be ascribed to the better ordering of **JK-217D** in the solid state in the presence of two hexyloxy chains. Therefore, the

overall parameters contributed to the best PCE values of **JK-216D** and **JK-217D** as 14.74 % and 14.73 %, respectively. The statistical data of perovskite solar cells containing the two new HTMs based on 85 identical devices are shown in Fig. S4 (ESI†) giving the average PCE values of 12.12 % and 11.18 %, respectively.

Table 2. Summary of photovoltaic parameters derived from *J-V* measurements of $CH_3NH_3PbI_3$ based devices.

HTM	J_{sc} (mAcm^{-2})	V_{oc} (V)	FF (%)	η (%)
JK-216D	21.754	0.969	69.92	14.74
JK-217D	21.226	0.964	71.94	14.73
Spiro-OMeTAD	21.105	1.002	72.48	15.33

Performance of organic-inorganic cells were measured with 0.16 cm^2 working area.

Figure 5b shows the incident-photon-to-current conversion efficiency (IPCE) spectra for the devices using the two JK-216D and JK-217D HTM's. The perovskite solar cells using JK-216D show an excellent photocurrent response from 300 to 800 nm, with the IPCE reaching a maximum of 82% at 490 nm, while spiro-OMeTAD and **JK-217D** based devices showed a maximum IPCE of 84% at 490 nm and 80% at 480 nm, respectively. Although the photoresponse of the device using the spiro-OMeTAD is slightly better than the squaraine-based HTMs below 600 nm, it is noticeable to see an improvement of the photocurrent between 680–800 nm due to the contribution of low bandgap squaraine. A shoulder at 740 nm with IPCE values of 65% correlated well with the absorption maximum in thin films (Figure 2b). This result proved the dual function of squaraine pigments as light harvesting and hole transporting layers inside the perovskite solar cells. Mismatch between the IPCE spectra and absorption spectra is observed and is ascribed to the electron transfer from the excited aggregates to the perovskite as well as from the monomers which have different quantum yields.[39,40]

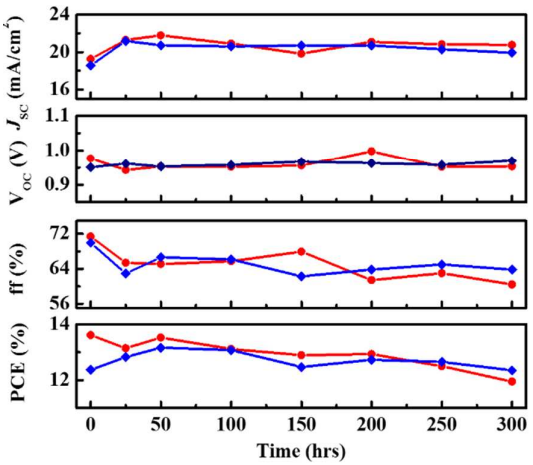

Figure 6. Stability test for devices based on **JK-216D** (●) and **JK-217D** ( ).

Finally, the operational stability of the squaraine-based perovskite solar cell was tested under light intensity of 100 mW cm^{-2} and the data are shown in Figure 6. The unsealed cells showed little change in J_{SC} and V_{OC} over time but the *ff* decreases more prominently. After 300 h in the ambient environment, the PCE of the device with JK216D as HTM keeps 88% of its initial value, however the JK217D exhibited almost no change, indicating a superior long-term stability of the JK217D.

Conclusions

In summary, we reported for the first time asymmetric squaraine-based low band-gap hole transporting material, which acted as both light harvesting and hole transporting layers in perovskite solar cells. Optoelectrochemical characterization revealed extremely high molar extinction absorption bands in the low energy region and prominent space charge delocalization due to its electronically asymmetric nature. Suitable bands alignments of the squaraine molecules with perovskite and photoanode allowed cascade electron injection and effective hole extraction in perovskite solar cells. Red-shifted absorption was observed for both HTMs in thin films coated on perovskite. The optimized devices exhibited an impressive

PCE of 14.7 % under full sunlight illumination (100 mW cm^{-2}, AM1.5 G), which is comparable to that of the devices using a state-of-the-art spiro-OMeTAD hole transport layer under similar conditions. Ambient stability after 300 h revealed that 88% of the energy conversion efficiency was kept for **JK216D** and almost no change with **JK217D**, indicating the devices had good long-term stability and thus suggesting that the asymmetric squaraine shows a great potential as a dual-functional HTM for high performance in perovskite solar cells.

Acknowledgments

This project was funded by the Deanship of Scientific Research (DSR), King Abdulaziz University, under grant No. (79-130-35-HiCi). The authors, therefore, acknowledge technical and financial support of KAU. MKN acknowledge funding from the European Union Seventh Framework Programme [FP7/2007-2013] under grant agreement n° 604032 of the MESO project, (FP7/2007-2013) ENERGY.2012.10.2.1; NANOMATCELL, grant agreement no. 308997. The National Research Foundation of Korea (NRF) grant funded by the Korea government (MSIP) No. 2014R1A2A2A03004716.

References

1. P. Gao, M. Grätzel, and M. K. Nazeeruddin, *Energy Environ. Sci.*, 2014, **7**, 2448.
2. M. D. McGehee, *Nat. Mater.*, 2014, **13**, 845–846.
3. W. S. Yang, J. H. Noh, N. J. Jeon, Y. C. Kim, S. Ryu, J. Seo, and S. Il Seok, *Science (80-.).*, 2015, **348**, 1234–1237.
4. C. C. Stoumpos, C. D. Malliakas, and M. G. Kanatzidis, *Inorg. Chem.*, 2013, **52**, 9019–9038.

5. H.-S. Kim, C.-R. Lee, J.-H. Im, K.-B. Lee, T. Moehl, A. Marchioro, S.-J. Moon, R. Humphry-Baker, J.-H. Yum, J. E. Moser, M. Grätzel, and N.-G. Park, *Sci. Rep.*, 2012, **2**, 591.

6. S. D. Stranks and H. J. Snaith, *Nat. Nanotechnol.*, 2015, **10**, 391–402.

7. Q. Dong, Y. Fang, Y. Shao, P. Mulligan, J. Qiu, L. Cao, and J. Huang, *Science (80-.).*, 2015, **347**, 967–970.

8. M. M. Lee, J. Teuscher, T. Miyasaka, T. N. Murakami, and H. J. Snaith, *Science (80-.).*, 2012, **338**, 643–647.

9. N. Ahn, D.-Y. Son, I.-H. Jang, S. M. Kang, M. Choi, and N.-G. Park, *J. Am. Chem. Soc.*, 2015, **137**, 8696–8699.

10. N. Jeon, H. Lee, Y. Kim, and J. Seo, *J. Am. Chem. Soc.*, 2014.

11. H. Li, K. Fu, P. P. Boix, L. H. Wong, A. Hagfeldt, M. Grätzel, S. G. Mhaisalkar, and A. C. Grimsdale, *ChemSusChem*, 2014, **7**, 3420–3425.

12. T. Krishnamoorthy, F. Kunwu, P. P. Boix, H. Li, T. M. Koh, W. L. Leong, S. Powar, A. Grimsdale, M. Grätzel, N. Mathews, and S. G. Mhaisalkar, *J. Mater. Chem. A*, 2014, **2**, 6305.

13. N. J. Jeon, J. H. Noh, Y. C. Kim, W. S. Yang, S. Ryu, and S. Il Seok, *Nat. Mater.*, 2014, **13**, 897–903.

14. J. H. Heo, S. H. Im, J. H. Noh, T. N. Mandal, C.-S. Lim, J. A. Chang, Y. H. Lee, H. Kim, A. Sarkar, M. K. Nazeeruddin, M. Grätzel, and S. Il Seok, *Nat. Photonics*, 2013, **7**, 486–491.

15. B. Cai, Y. Xing, Z. Yang, W.-H. Zhang, and J. Qiu, *Energy Environ. Sci.*, 2013, **6**, 1480.

16. Y. S. Kwon, J. Lim, H.-J. Yun, Y.-H. Kim, and T. Park, *Energy Environ. Sci.*, 2014, **7**, 1454.

17. Q. Lin, A. Armin, R. C. R. Nagiri, P. L. Burn, and P. Meredith, *Nat. Photonics*, 2014, **9**, 106–112.

18. P. Qin, H. Kast, M. K. Nazeeruddin, S. M. Zakeeruddin, A. Mishra, P. Bauerle, and M. Gratzel, *Energy Environ. Sci.*, 2014, **7**, 2981–2985.

19. Y. Liu, Q. Chen, H.-S. Duan, H. Zhou, Y. (Michael) Yang, H. Chen, S. Luo, T.-B. Song, L. Dou, Z. Hong, and Y. Yang, *J. Mater. Chem. A*, 2015, **3**, 11940–11947.

20. C. Steck, M. Franckevičius, S. M. Zakeeruddin, A. Mishra, P. Bäuerle, and M. Grätzel, *J. Mater. Chem. A*, 2015.

21. F. Javier Ramos, M. Ince, M. Urbani, A. Abate, M. Grätzel, S. Ahmad, T. Torres, and M. K. Nazeeruddin, *Dalt. Trans.*, 2015, **44**, 10847–10851.

22. P. Qin, S. Paek, M. I. Dar, N. Pellet, J. Ko, M. Grätzel, and M. K. Nazeeruddin, *J. Am. Chem. Soc.*, 2014, **136**, 8516–8519.

23. W. Ziegenbein and H.-E. Sprenger, *Angew. Chemie Int. Ed. English*, 1966, **5**, 893–894.

24. C. Qin, W.-Y. Wong, and L. Han, *Chem. Asian J.*, 2013, **8**, 1706–19.

25. D. Bagnis, L. Beverina, H. Huang, F. Silvestri, Y. Yao, H. Yan, G. a. Pagani, T. J. Marks, and A. Facchetti, *J. Am. Chem. Soc.*, 2010, **132**, 4074–4075.

26. Y. Chen, Z. Zeng, C. Li, W. Wang, X. Wang, and B. Zhang, *New J. Chem.*, 2005, **29**, 773.

27. H. Choi, S. Kim, S. O. Kang, J. Ko, M.-S. Kang, J. N. Clifford, A. Forneli, E. Palomares, M. K. Nazeeruddin, and M. Grätzel, *Angew. Chemie Int. Ed.*, 2008, **47**, 8259–8263.

28. J.-Y. Li, C.-Y. Chen, W.-C. Ho, S.-H. Chen, and C.-G. Wu, *Org. Lett.*, 2012, **14**, 5420–3.

29. M. Gsänger, E. Kirchner, M. Stolte, C. Burschka, V. Stepanenko, J. Pflaum, and F. Würthner, *J. Am. Chem. Soc.*, 2014, **136**, 2351–2363.

30. S. Paek, H. Choi, C. Kim, N. Cho, S. So, K. Song, M. K. Nazeeruddin, and J. Ko, *Chem. Commun. (Camb).*, 2011, **47**, 2874–6.

31. L. Etgar, P. Gao, Z. Xue, Q. Peng, A. K. Chandiran, B. Liu, M. K. Nazeeruddin, and M. Grätzel, *J. Am. Chem. Soc.*, 2012, **134**, 17396–17399.

32. N. J. Jeon, H. G. Lee, Y. C. Kim, J. Seo, J. H. Noh, J. Lee, and S. Il Seok, *J. Am. Chem. Soc.*, 2014, **136**, 7837–7840.

33. F. M. Jradi, X. Kang, D. O'Neil, G. Pajares, Y. a. Getmanenko, P. Szymanski, T. C. Parker, M. a. El-Sayed, and S. R. Marder, *Chem. Mater.*, 2015, **27**, 2480–2487.

34. Z. S. Wang, K. Hara, Y. Dan-oh, C. Kasada, A. Shinpo, S. Suga, H. Arakawa, and H. Suglhara, *J. Phys. Chem. B*, 2005, **109**, 3907–3914.

35. P. Qin, N. Tetreault, M. I. Dar, P. Gao, K. L. Mccall, S. R. Rutter, S. D. Ogier, N. D. Forrest, J. S. Bissett, M. J. Simms, A. J. Page, R. Fisher, M. Grätzel, and M. K. Nazeeruddin, *Adv. Energy Mater.*, 2014, **197**, n/a–n/a.

36. A. Krishna, D. Sabba, H. Li, J. Yin, P. P. Boix, C. Soci, S. G. Mhaisalkar, and A. C. Grimsdale, *Chem. Sci.*, 2014, **5**, 2702.

37. P. Ganesan, K. Fu, P. Gao, I. Raabe, K. Schenk, R. Scopelliti, J. Luo, L. H. Wong, M. Grätzel, and M. K. Nazeeruddin, *Energy Environ. Sci.*, 2015, **8**, 1986–1991.

38. A. Abate, S. Paek, F. Giordano, J.-P. Correa-Baena, M. Saliba, P. Gao, T. Matsui, J. Ko, S. M. Zakeeruddin, K. H. Dahmen, A. Hagfeldt, M. Grätzel, and M. K. Nazeeruddin, *Energy Environ. Sci.*, 2015.

39. A. Ehret, L. Stuhl, and M. T. Spitler, *J. Phys. Chem. B*, 2001, **105**, 9960–9965.

40. K. Sayama, S. Tsukagoshi, K. Hara, Y. Ohga, A. Shinpou, Y. Abe, S. Suga, and H. Arakawa, *J. Phys. Chem. B*, 2002, **106**, 1363–1371.